Anomalous glass transition behavior of SBR–Al_2O_3 nanocomposites at small filler concentrations

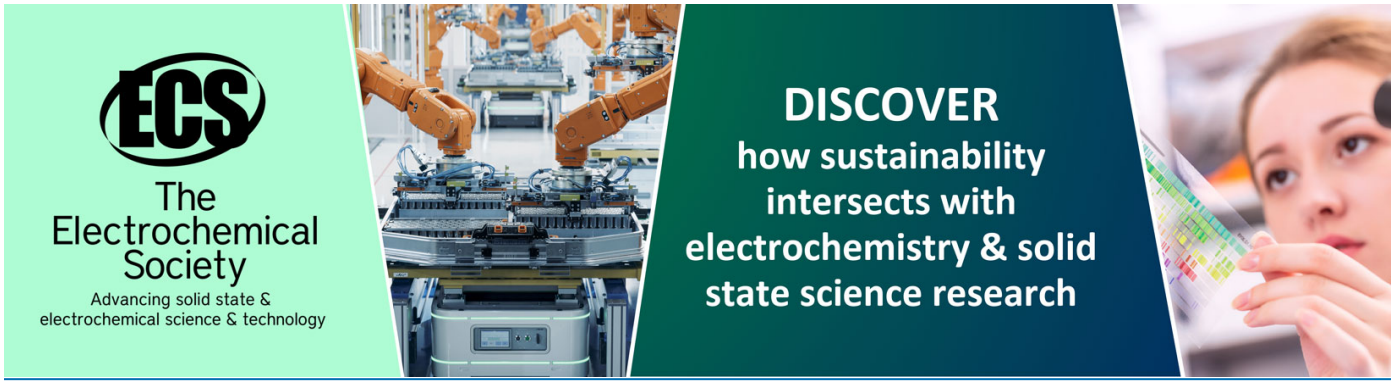

OPEN ACCESS
IOP Publishing
Nanotechnology

Nanotechnology **25** (2014) 425704 (8pp)
doi:10.1088/0957-4484/25/42/425704

Anomalous glass transition behavior of SBR–Al_2O_3 nanocomposites at small filler concentrations

Rymma Sushko, Marlena Filimon, Rick Dannert, Patrick Elens, Roland Sanctuary and Jörg Baller

Physics and Materials Science Research Unit, Laboratory for the Physics of Advanced Materials, University of Luxembourg, 162A avenue de la Faïencerie, L-1511, Luxembourg

E-mail: joerg.baller@uni.lu

Received 12 May 2014, revised 8 August 2014
Accepted for publication 28 August 2014
Published 3 October 2014

Abstract

Elastomers filled with hard nanoparticles are of great technical importance for the rubber industry. In general, fillers improve mechanical properties of polymer materials, e.g. elastic moduli, tensile strength etc. The smaller the size of the particles, the larger is the interface where interactions between polymer molecules and fillers can generate new properties. Using temperature-modulated differential scanning calorimetry and dynamic mechanical analysis, we investigated the properties of pure styrene-butadiene rubber (SBR) and SBR/alumina nanoparticles. Beside a reinforcement effect seen in the complex elastic moduli, small amounts of nanoparticles of about 2 wt% interestingly lead to an acceleration of the relaxation modes responsible for the thermal glass transition. This leads to a minimum in the glass transition temperature as a function of nanoparticle content in the vicinity of this critical concentration. The frequency dependent elastic moduli are used to discuss the possible reduction of the entanglement of rubber molecules as one cause for this unexpected behavior.

Keywords: nanocomposites, styrene-butadiene, alumina, nanoparticles, glass transition, DMA, TMDSC

(Some figures may appear in colour only in the online journal)

1. Introduction

Nowadays, many research works are dedicated to the modification of polymer properties using nanometer sized fillers [1, 3, 13, 16, 28, 30]. The improvement of mechanical properties of polymers [13, 14, 16, 18, 29, 30] is important for many applications, e.g. reinforcement of elastomers [17] for the use in car tires. In filled polymers, the mobility of polymer molecules is often reduced. This can be due to e.g. confinement effects by the fillers or due to interactions between polymer molecules and filler particles. This effect is usually more pronounced for nanometer sized fillers than for micrometer sized fillers [28, 30]. The reduced mobility often leads to increased glass transition temperatures [7, 10, 19–21, 23, 26]. The introduction of fillers into a polymer matrix is generally accompanied by the formation of layers (interphases) of slowed molecular dynamics around the particles [2, 9, 12, 25, 26]. In elastomers, interphases with almost immobile molecules are known as bound rubber [19]. If the difference in mobility between molecules in the interphase and the bulk is high enough, two glass transitions have also been reported [2, 25, 26]. Depending on the interaction between fillers and matrix molecules, unchanged [5, 22] or even accelerated [9] molecular dynamics can be found too (for a decent review please see [11]). The sign of the filler influence on the mobility of polymer molecules may even depend on the molecular weight of the matrix molecules [8].

Most of the studies analyze the effect of high nanoparticle concentrations up to 50 wt% on the composites' properties. Nevertheless, even at small filler contents, changed molecular mobility leading to changes in the glass transition behavior has been reported [8–10]. With the exception of the work of Bindu *et al* [10], it is common for all studies cited above, that the incorporation of nanoparticles influences the glass transition temperatures for a given system only in one way (increase, decrease or no change). In the present work, we present a system (styrene-butadiene rubber (SBR) filled with untreated alumina nanoparticles) where both accelerated as well as reduced molecular dynamics can be found for the same system. This leads to a minimum in the glass transition temperature at small filler concentrations. Dynamic mechanical analysis (DMA), rheometry and temperature-modulated differential scanning calorimetry (TMDSC) together with structural investigation tools have been used to shed light on this unexpected experimental finding.

2. Experimental

2.1. Materials

Poly(styrene-co-butadiene) rubber (SBR, Sigma-Aldrich) containing 45% of styrene and alumina nanoparticles (Aeroxide Alu C delivered by Evonik) were used in this work. According to the producer, the average diameter of the primary particles produced by noble gas condensation is about 13 nm. During the production process, primary particles sinter into irregularly shaped, chemically bonded aggregates. This leads to fractal nanoparticles with linear dimensions between 13 and 200 nm [6]. The solvent used in this work (chloroform) is of spectroscopic purity grade, supplied by Carl Roth GmbH.

2.2. Composite preparation and characterization

To produce the SBR/AluC nanocomposites, the following procedure was used [4]: a known mass of AluC nanoparticles was dispersed and sonicated in chloroform, after which a known quantity of 10% SBR solution in chloroform was injected. This mixture was stirred in a planetary mixer for 15 min and then freeze–dried. The samples for investigations were molded into disks in a vacuum oven at 85 °C during 24 h.

Thus, a series of disk-like nanocomposites containing 1, 1.5, 2, 3, 4, 10 and 20 wt% of AluC nanoparticles was prepared. To examine the dispersion of the alumina nanoparticles in the SBR matrix, cross-section samples were cut using a microtome. The cross-sectioned areas were examined by transmission electron microscopy (TEM). The TEM (JEOL JEM 2011-HRTEM) was operated at an acceleration voltage of 100 kV. Figure 1 shows TEM pictures of SBR samples filled with 1, 2 and 4 wt% of alumina nanoparticles at four different magnifications. The highest magnification of the 1% sample depicts the chemical aggregation of the primary particles (13 nm) to fractal nanoparticles (up to 200 nm in diameter). It has been shown that these aggregates cannot be broken even by high shear forces [27]. The higher concentrations (2% and 4%) show the formation of small agglomerates of aggregates. Prior investigations have shown [7] that these agglomerates can easily be broken by applying shear forces, e.g. in AluC/epoxy resin nanocomposites. Therefore we assume that the agglomerates are held together by small Van der Waals forces due to the hydrophilic nature of the aluminas' surfaces.

To ensure the right filler concentrations especially at low filler contents, degradation experiments between 300 and 770 K were performed using thermogravimetric analysis (TGA, TA Instruments TGA 2590) (figure 2).

2.3. Techniques

Temperature-modulated differential scanning calorimetry (TMDSC, Mettler Toledo DSC 823) was used to investigate the glass transition behavior of the SBR nanocomposites. Samples of 6–10 mg were weighed and sealed in aluminum pans. TMDSC measurements were performed in nitrogen atmosphere in the temperature range from 298 to 223 K with a cooling rate of 0.5 K min^{-1}, a temperature modulation amplitude of 0.5 K and a modulation period of 2 min. The real and imaginary parts of the specific heat capacity were evaluated using standard methods [24]. The glass transition temperature was determined as the inflection point of the real part of the specific heat capacity. Temperature and heat flow calibration of the calorimeter was done using adamantane, water, indium, naphthalene, benzoic acid and zinc standards.

The viscoelastic behavior of the samples was characterized at low strains (linear regime conditions) using DMA (Mettler Toledo DMA/SDTA 861e). Two equal disks of each nanocomposite with diameters of about 8 mm and thicknesses of about 1 mm were mounted into a shearing device. The storage G' and loss G'' parts of the dynamic shear modulus were isothermally measured as a function of frequency (from 0.008 to 800 Hz) at the following temperatures: 223, 233, 243, 253, 273, 293, 313, 333, 353 and 373 K. The DMA method is limited by the fact that the sample holder can only poorly be adapted to the changing thickness of the sample. This holds especially true at low temperatures (high frequencies in the master curves) near or below the thermal glass transition. To overcome this problem, rheometry (Anton Paar MCR 302 rheometer) was also performed on disc-like samples in parallel plate geometry (diameter 8 mm). For more details of the experimental setup see [15]. During the rheological measurements, the normal force was kept constant at 2 N and the gap size (usually between 1 and 2 mm) was allowed to adapt to the thermal expansion of the samples. Using this configuration, we were able to measure loss curves ($\tan\delta$) in the region of the dynamic glass transition (figure 9). The rheology measurements were made by isothermal frequency sweeps at 238, 243, 248, 253, 263, 273, 283, 288, 303, 303, 323 and 343 K. The measurement conditions were always chosen to strictly respect the linear response regime for each frequency f and at any given temperature T.

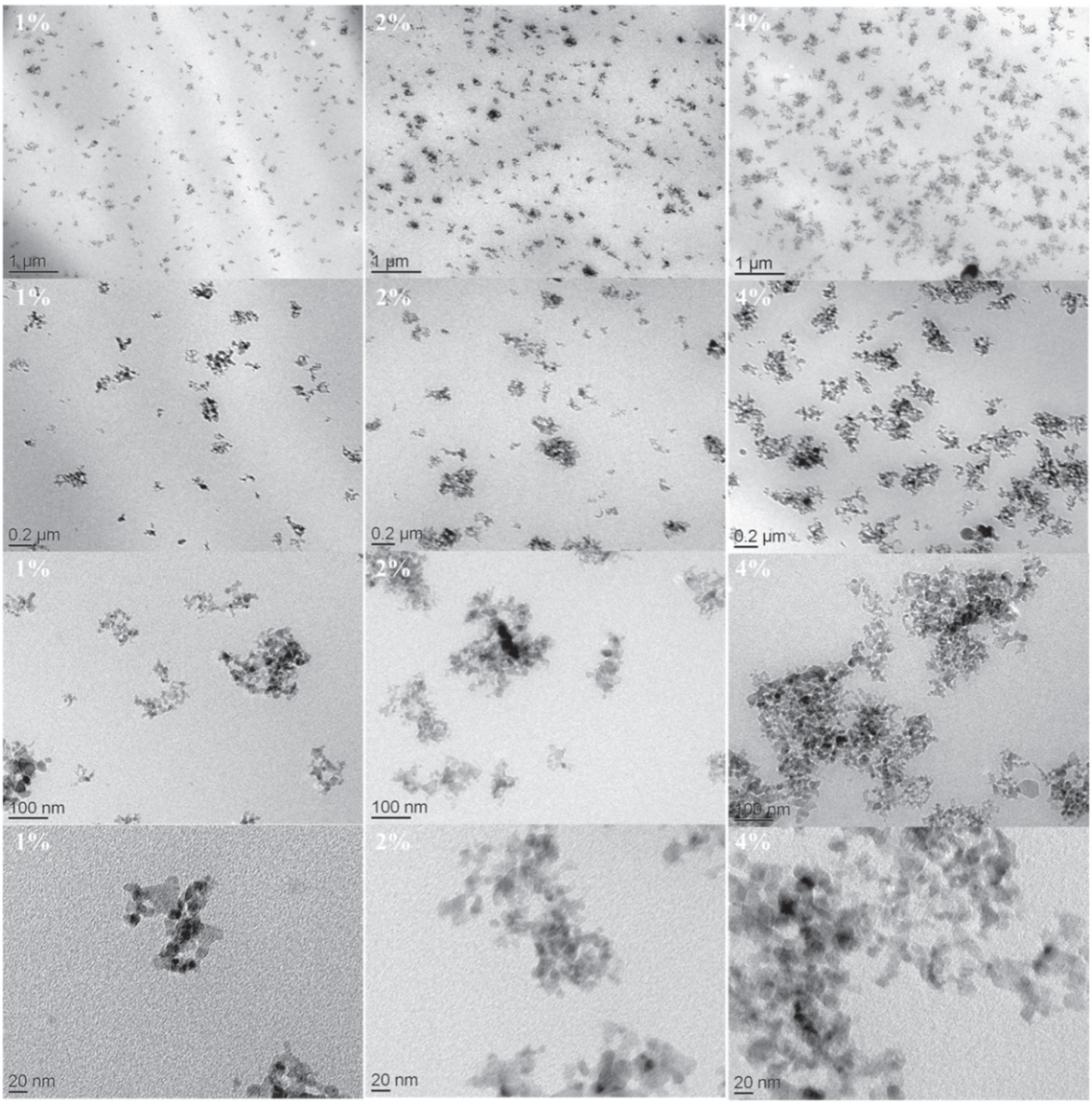

Figure 1. TEM pictures of the SBR nanocomposites with 1% (left), 2% (middle) and 4% (right) of alumina nanoparticles.

3. Results and discussion

3.1. Results from calorimetry

The upper part of figure 3 shows the glass transition temperatures T_g of the SBR/Alu C composites for different filler concentrations. The most prominent feature is an unexpected minimum in T_g at $w_{AluC} \approx 1.5$–2 wt%.

The slight increase of T_g from the pure SBR system to the system filled with 20 wt% of alumina nanoparticles measures up to expectations: (i) the mere presence of the nanoparticles hinders the flow/movement of the polymer molecules, (ii) interactions between SBR molecules and the nanoparticles' surfaces are expected to slow down the molecular dynamics of the composite system. As the change of T_g remains small for high filler loading ($w_{AluC} > 10$ wt%), it can be suggested that the molecular mobility of the chains is only moderately slowed down by the new interactions promoted between the hydrophilic fillers and the hydrophobic matrix molecules. The unexpected minimum in T_g signifies an acceleration of the dynamics of the SBR molecules for low filler concentrations compared to the pure SBR system.

3.2. Results from mechanical spectroscopy

Dynamic mechanical investigations were conducted to examine the effect of nanofillers on the thermomechanical properties of SBR nanocomposites. Figure 4 shows master curves of the storage modulus $G'(f)$ and loss modulus $G''(f)$ for composites with different concentrations of alumina nanoparticles. As an overview, figure 4 shows the effect of the incorporation of nanoparticles on the G' and G'' curves for the systems containing 0%, 10% and 20% Alu C. These systems obviously present noticeable reinforcement effect. The master curves (figure 4) display four different regions which are characteristic for the viscoelastic behavior of

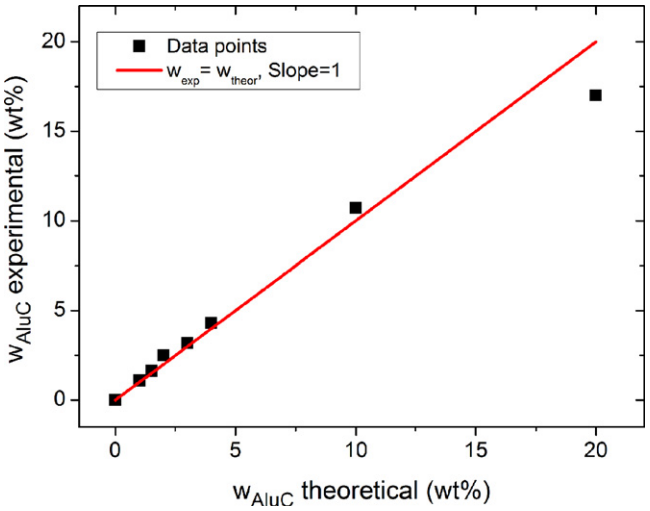

Figure 2. Experimental AluC concentration w_{AluC} determined by thermogravimetry versus theoretical AluC concentration for the nanocomposites under study.

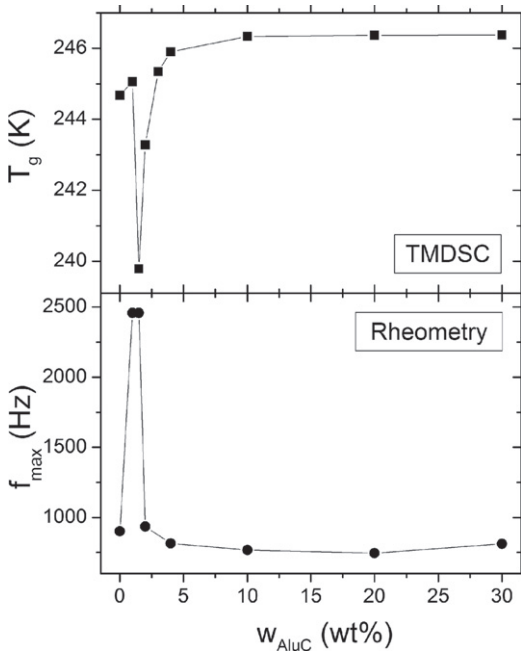

Figure 3. Glass transition temperatures T_{g} from the real part of the specific heat capacity (measured at 8.3 mHz with TMDSC) and frequency positions of the maxima of the tan δ curves (at 273 K from rheology, figure 9) as a function of nanoparticle content.

rubber-like materials: (i) the glassy region in the high frequency range where the composites are dynamically frozen; (ii) the transition zone between glass and rubber where the mechanic properties are dominated by the structural relaxation processes connected to the dynamic freezing; (iii) the rubbery plateau where the slope of the master curves is reduced due to physical cross-links by entanglement of SBR molecules; (iv) the terminal flow range at low frequencies.

Figure 5 shows the influence of the nanoparticles on the elastic moduli in the region around the rubbery plateau in more detail. To construct the master curves for a reference temperature of 273 K, the temperature–frequency equivalence principle has been exploited. The corresponding horizontal shift factors log a_T for all nanocomposite systems are depicted in figure 6. No vertical shift was necessary ($b_{\mathrm{T}} = 1$). The shape of the log a_{T} curves does not vary much with the nanoparticle content. This means that the temperature dependencies of the intrinsic relaxation processes are qualitatively the same for all nanoparticle concentrations.

In the glassy region, the effect of the nanoparticles is less pronounced than in the other regions. This is due to the fact that the stiffness moduli of the SBR matrix approach the high moduli of the alumina nanoparticles at high frequencies. In all other regions, the reinforcement effect of the nanoparticles can clearly be seen in the frequency dependency of both master curves.

The reinforcement effect is also found for small nanoparticle concentrations below 10 wt%, but figure 5 shows that there is a dependency of this effect on the probe frequency. Figures 7 and 8 resolve this dependency for both the real part (figure 7) as well as for the imaginary part (figure 8) of the complex elastic modulus measured by DMA.

The $G'(w_{\mathrm{AluC}})$ curve for 10^{-4} Hz shows a reinforcement effect which increases with the concentration of nanoparticles. This general trend is observed up to a frequency of about 10 Hz. For higher frequencies approaching the dynamic glass transition, the reinforcement increases rapidly at low concentrations—almost showing a maximum at about $w_{\mathrm{AluC}} = 1.5$ wt%. The same behavior can be observed for the $G''(w_{\mathrm{AluC}})$ curves. The maximum at about $w_{\mathrm{AluC}} = 1.5$ wt% is even more pronounced. Comparing the concentration dependency of both moduli with the filler content dependency of the thermal glass transition temperature (figures 7 and 8), it turns out that the maximum in the moduli is found at the same nanoparticle concentration as the minimum in T_{g}.

3.3. Discussion

The most prominent feature of the presented experimental results is the minimum in the glass transition temperature T_{g} of the nanocomposites for low filler concentrations. This minimum is accompanied by a general trend towards increasing T_{g} values with increasing nanoparticle concentration. It can only be explained by a mechanism or process which accelerates the dynamics of the rubber molecules for filler concentrations up to about 2 wt%. This would be the opposite of what is known as 'bound rubber' [19]. Since the untreated alumina nanoparticles have a hydrophilic character, it could be argued that the hydrophobic rubber molecules show only weak interactions with the nanoparticles' surfaces leading to accelerated dynamics of rubber molecules near nanoparticle surfaces. This should however also be the case for higher filler concentrations leading to a general trend to lower glass transition temperatures which is at first sight in contradiction to the experimental findings. However, Bindu *et al* [10] argue for natural rubber/ZnO nanocomposites that, starting at concentrations of about 2 vol%, aggregation of nanoparticles takes place leading to a preference of nanoparticle/nanoparticle interactions over nanoparticle/rubber

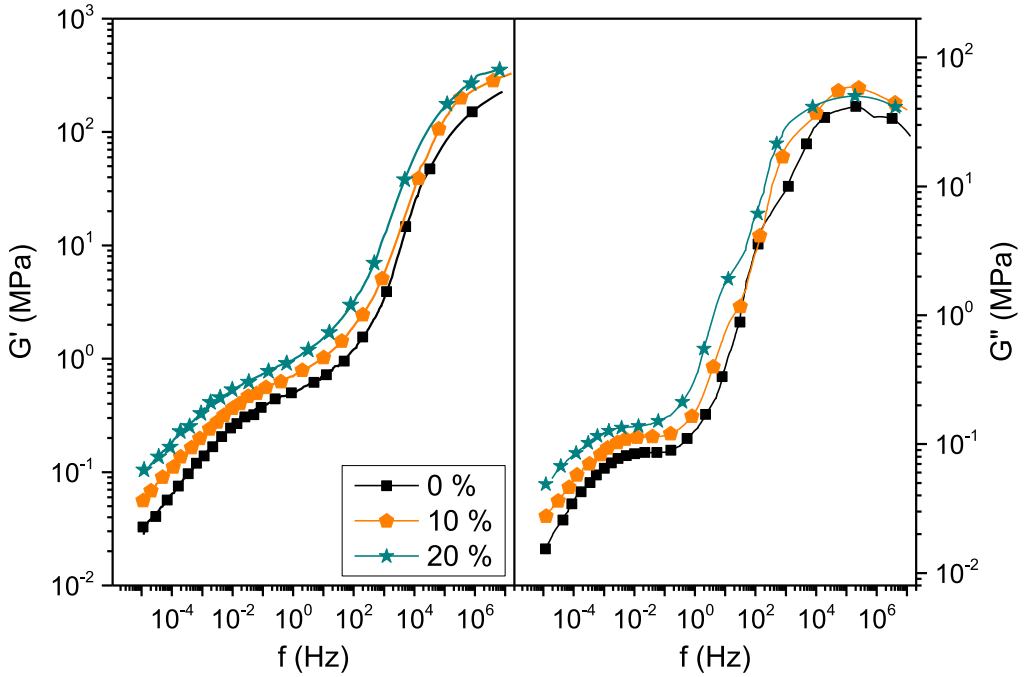

Figure 4. Master curves of the elastic moduli for selected nanocomposites (see text). Symbols are only used for the sake of clarity; data points lie much closer (figure 5) and are here represented by solid lines. DMA measurements, reference temperature: 273 K.

interactions. Our TEM data (figure 1) shows a slight tendency for the nanoparticles to cluster, but this tendency can be found for all of the samples investigated by TEM (1%, 2% and 4%). The sample with 2% does not show any peculiarities. Furthermore, experiments with SBR nanocomposites with the same alumina particles but coated with several different hydrophobic layers (to be published) show a similar T_g minimum at low filler concentrations. This leads us to the conclusion that aggregation of nanoparticles is not the reason for the observed behavior. Moreover we claim that the reduction of the number of entanglements (physical cross-links) between polymer chains by the presence of small amounts of nanoparticles is responsible for the accelerated local dynamics at small filler concentrations. During the preparation of the nanocomposites from solution, the nanoparticles seem to hinder the formation of physical cross-links. The structural relaxation (α-process) of the SBR molecules becomes faster which explains the decrease of T_g for these small concentrations. Since the number of entanglements in unfilled SBR rubber is limited, there is also a limit for the acceleration of the molecular dynamics. The accelerated dynamics at low concentrations is superimposed by a general trend to lower local dynamics with increasing filler concentration. This could be due to the fact that interactions at the nanoparticles' surfaces have a small retardation effect on the glass forming dynamics of the SBR molecules. This effect seems to be far too small to talk of 'bound rubber': the increase of T_g from unfilled to 20 wt% is only about 1.7 K! In addition to possible attractive interactions between rubber molecules and nanoparticle surfaces, confinement of the rubber molecules by the presence of the nanoparticles could also be the reason for the slight overall increase of the glass transition temperature.

Measurements of the loss factor $\tan\delta$ by rheology support the idea of increased (at about 1.5–2%) and slowed (>4%) mobility: in the upper part of figure 9, the frequency dependence of $\tan\delta$ at a reference temperature of 273 K is shown. The lower part shows the same curves scaled vertically by a factor in a way that all curves have the same height at the maximum. There are two important results: (i) The shift of a single $\tan\delta$ curve with a specific nanoparticle concentration with regard to the curve of the unfilled rubber is the same at all frequencies shown in figure 9. This means that the influence of the nanoparticles on the dynamics of the rubber molecules is the same for low frequencies where flow plays a major role and for high frequencies around the dynamic glass transition temperature where segmental mobility dominates. This holds true for the curves which are shifted to higher frequencies as well as for curves shifted to lower frequencies. (ii) The shift of the $\tan\delta$ maximum with the concentration of the nanoparticles, i.e. the dynamic glass transition at the reference temperature of 273 K, reflects the results of the TMDSC measurements: in the lower part of figure 3, the frequencies of the $\tan\delta$ maximum are plotted as a function of filler content. At the concentrations where the T_g values show a minimum, the $\tan\delta$ data shows a maximum. Using the activation plot of the α-process measured by dielectric spectroscopy for the pure SBR system, it can be calculated that the 8.3 mHz at T_g from the TMDSC measurements corresponds to about 300 Hz at the reference temperature of 273 K used for the master curves of the $\tan\delta$ data. From the fact, that the concentration dependent shift of the $\tan\delta$ curves is independent of the frequency (see (i)), it can be expected that the T_g minimum from TMDSC measurements can be found

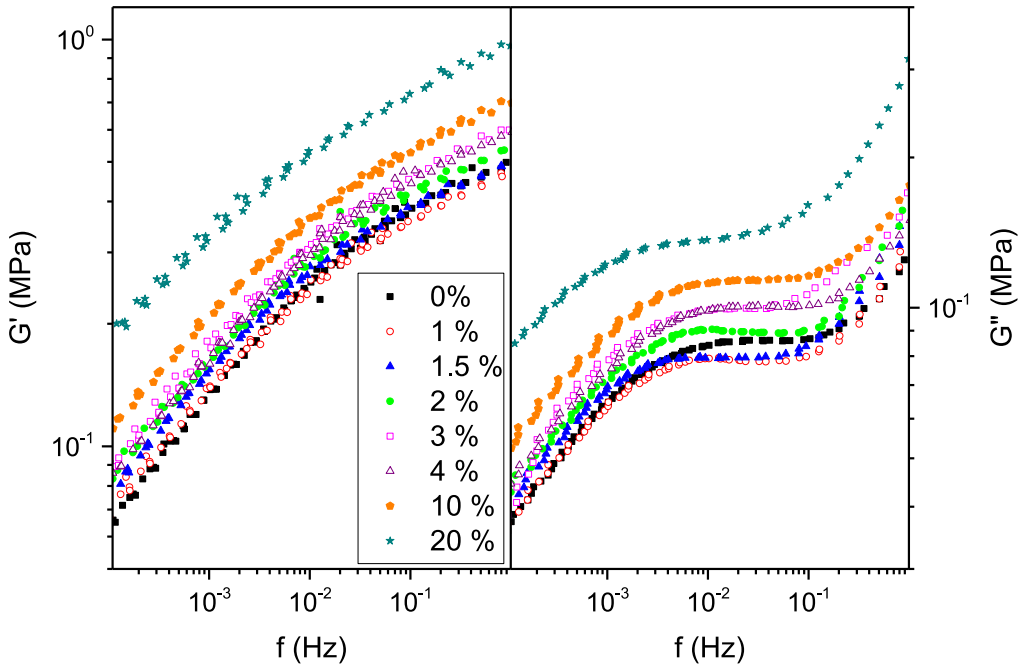

Figure 5. Master curves of the elastic moduli of all nanocomposites in a frequency region around the rubbery plateau. DMA measurements, reference temperature: 273 K.

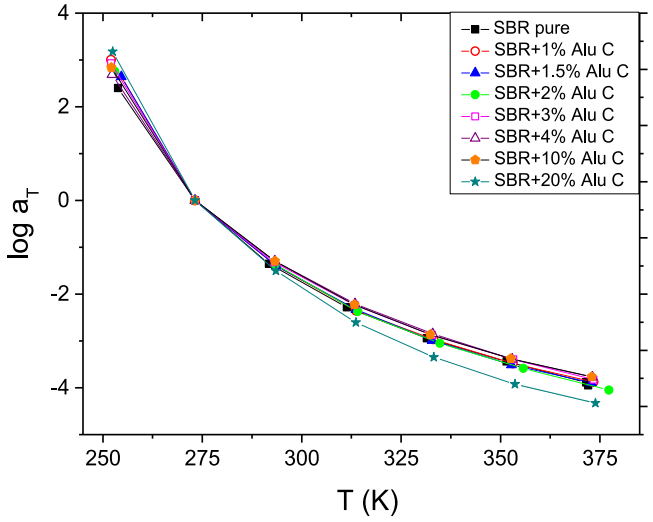

Figure 6. Horizontal shift factors log a_T used to construct the master curves displayed in figures 4 and 5. DMA measurements, reference temperature: 273 K.

at the same nanoparticles concentration as the maximum of the tan δ curves.

To summarize, acceleration due to reduction of entanglements on one hand and retardation due to nanoparticle/rubber interactions and confinement on the other hand are made responsible for the unexpected behavior of the glass transition temperature from TMDSC and the loss maximum from rheology.

The effect of the disentanglement can be seen in both moduli (figures 7 and 8): there is a step at filler concentrations where the influence of disentanglement is expected to end.

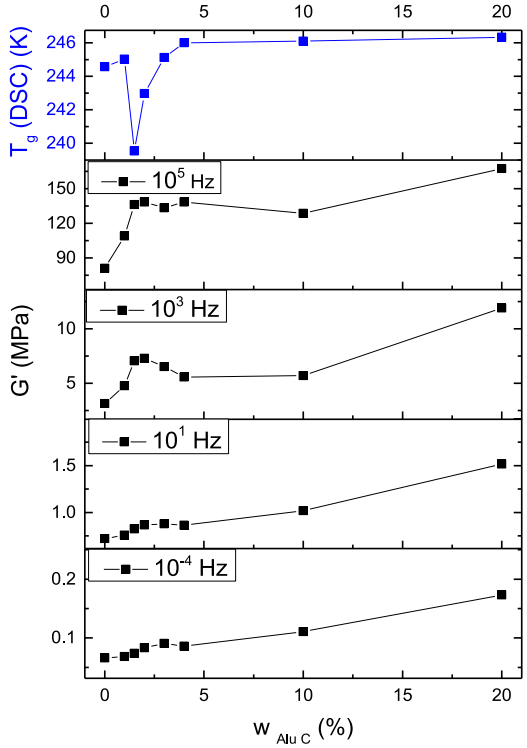

Figure 7. Storage modulus G' (DMA measurements) as a function of nanoparticle content, evaluated at different frequencies at the reference temperature of 273 K. Lines are guides for the eyes. The uppermost curve on the left side shows the dependency of the glass transition temperature of the nanoparticle content as measured by TMDSC.

4. Conclusions

Nanocomposites of untreated alumina nanoparticles and uncured SBR rubber were prepared and their thermal and

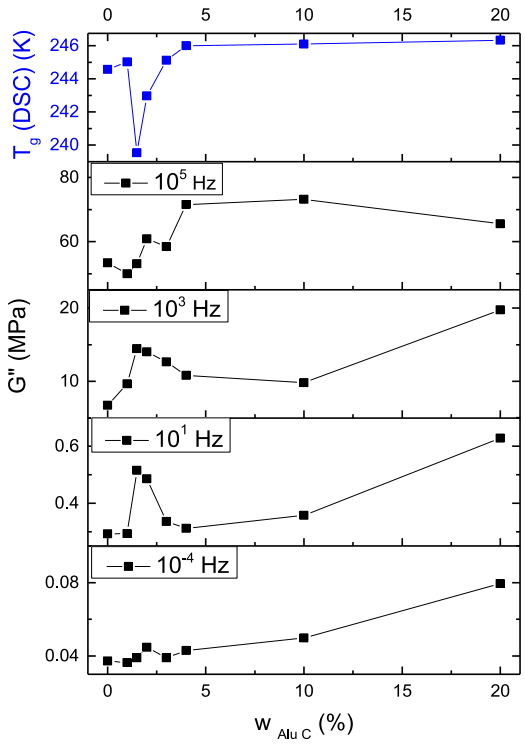

Figure 8. Loss modulus G'' (DMA measurements) as a function of nanoparticle content, evaluated at different frequencies at the reference temperature of 273 K. Lines are guides for the eyes. The uppermost curve on the left side shows the dependency of the glass transition temperature of the nanoparticle content as measured by TMDSC.

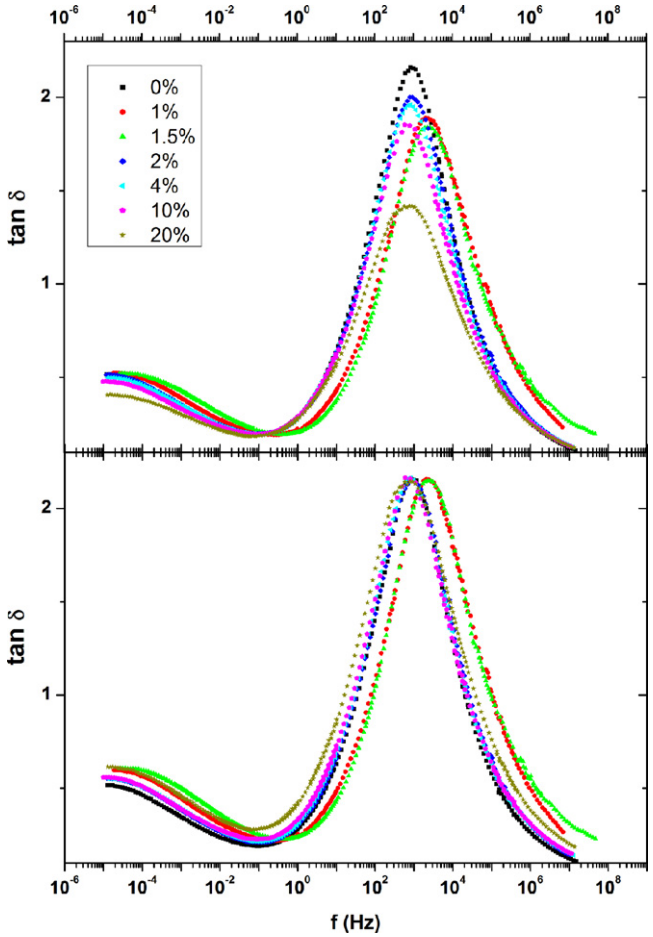

Figure 9. Master curves of tan δ from rheology. Reference temperature: 273 K.

dynamic mechanical properties were investigated by calorimetry and mechanical spectroscopy. An unexpected minimum in the glass transition temperature at small filler concentrations could be found. Two opposed processes are made responsible for the observed behavior: the underlying trend to higher glass transition temperatures with higher nanoparticle content is attributed to weak nanoparticle/rubber interactions and to confinement effects. Acceleration of molecular dynamics is considered as being a consequence of a reduction of the number of entanglements due to the presence of the nanoparticles during sample preparation from solution. This accelerating influence is limited by the total amount of entanglements present in the neat SBR. More investigations with different surface treatments of the nanoparticles are under way. First results confirm the presented minimum of the glass transition temperature for all of these systems. In our view, this supports the interpretation of the acceleration of the structural relaxation process being a consequence of disentanglement caused by the nanoparticles.

Acknowledgements

This work was kindly supported by the Fonds National de la Recherche Luxembourg. We thank Jörg Schmauch from the Universität des Saarlandes, Germany, for support with the TEM measurements. We thank the Goodyear Innovation Center Luxembourg for continuing support.

References

[1] Alexandre M and Dubois P 2000 Polymer-layered silicate nanocomposites: preparation, properties and uses of a new class of materials *Mater. Sci. Eng.* **28** 1–63

[2] Arrighi V, McEwen I J, Qian H and Prieto M B S 2003 The glass transition and interfacial layer in styrene-butadiene rubber containing silica nanofiller *Polymer* **44** 6259–66

[3] Balazs A C, Emrick T and Russell T P 2006 Nanoparticle polymer composites: where two small worlds meet *Science* **314** 1107–10

[4] Ballav N and Biswas M 2003 Preparation and evaluation of a nanocomposite of polythiophene with Al_2O_3 *Polym. Int.* **52** 179–84

[5] Baller J, Becker N, Ziehmer M, Thomassey M, Zielinski B, Müller U and Sanctuary R 2009 Interactions between silica nanoparticles and an epoxy resin before and during network formation *Polymer* **50** 3211–9

[6] Baller J, Thomassey M, Ziehmer M and Sanctuary R 2011 The catalytic influence of alumina nanoparticles on epoxy curing *Thermochim. Acta* **517** 34–9

[7] Baller J, Thomassey M, Ziehmer M and Sanctuary R 2011 *Thermoplastic and Thermosetting Polymers and Composites*

ed L D Tsai and M R Hwang (Hauppauge: Nova Science Publishers) 197–212
[8] Bansal A, Yang H, Li C, Benicewicz R C, Kumar S K and Schadler L S 2006 Controlling the thermornechanical properties of polymer nanocomposites by tailoring the polymer–particle interface *J. Polym. Sci. B* **44** 2944–50
[9] Bansal A, Yang H C, Li C Z, Cho K W, Benicewicz B C, Kumar S K and Schadler L S 2005 Quantitative equivalence between polymer nanocomposites and thin polymer films *Nat. Mater.* **4** 693–8
[10] Bindu P and Thomas S 2013 Viscoelastic behavior and reinforcement mechanism in rubber nanocomposites in the vicinity of spherical nanoparticles *J. Phys. Chem.* B **117** 12632–48
[11] Cangialosi D, Boucher V M, Alegria A and Colmenero J 2013 Physical aging in polymers and polymer nanocomposites: recent results and open questions *Soft Matter* **9** 8619–30
[12] Ciprari D, Jacob K and Tannenbaum R 2006 Characterization of polymer nanocomposite interphase and its impact on mechanical properties *Macromolecules* **39** 6565–73
[13] Coleman J N, Khan U and Gun'ko Y K 2006 Mechanical reinforcement of polymers using carbon nanotubes *Adv. Mater.* **18** 689–706
[14] Daniel I M, Miyagawa H, Gdoutos E E and Luo J J 2003 Processing and characterization of epoxy/clay nanocomposites *Exp. Mech.* **43** 348–54
[15] Dannert R, Sanctuary R, Thomassey M, Elens P, Krüger J K and Baller J 2014 Strain-induced low-frequency relaxation in colloidal DGEBA/SiO2 suspensions *Rheolo. Acta* doi:10.1007/s00397-014-0788-9
[16] Evora V M F and Shukla A 2003 Fabrication, characterization, and dynamic behavior of polyester/TiO_2 nanocomposites *Mater. Sci. Eng. A* **361** 358–66
[17] Gauthier C, Reynaud E, Vassoille R and Ladouce-Stelandre L 2004 Analysis of the non-linear viscoelastic behaviour of silica filled styrene butadiene rubber *Polymer* **45** 2761–71
[18] Guo Z H, Pereira T, Choi O, Wang Y and Hahn H T 2006 Surface functionalized alumina nanoparticle filled polymeric nanocomposites with enhanced mechanical properties *J. Mater. Chem.* **16** 2800–8
[19] Heinrich G, Kluppel M and Vilgis T A 2002 Reinforcement of elastomers *Curr. Opin. Solid State Mater. Sci.* **6** 195–203
[20] Lee A and Lichtenhan J D 1998 Viscoelastic responses of polyhedral oligosilsesquioxane reinforced epoxy systems *Macromolecules* **31** 4970–4
[21] Priestley R D, Rittigstein P, Broadbelt L J, Fukao K and Torkelson J M 2007 Evidence for the molecular-scale origin of the suppression of physical ageing in confined polymer: fluorescence and dielectric spectroscopy studies of polymer–silica nanocomposites *J. Phys.: Condens. Matter* **19** 2996
[22] Robertson C G, Lin C J, Rackaitis M and Roland C M 2008 Influence of particle size and polymer–filler coupling on viscoelastic glass transition of particle-reinforced polymers *Macromolecules* **41** 2727–31
[23] Sanctuary R, Baller J, Zielinski B, Becker N, Kruger J K, Philipp M, Muller U and Ziehmer M 2009 Influence of Al2O3 nanoparticles on the isothermal cure of an epoxy resin *J. Phys.: Condens. Matter* **21** 035118
[24] Schawe J E K 1995 A comparison of different evaluation methods in modulated temperature DSC *Thermochim. Acta* **260** 1–16
[25] Tsagaropoulos G and Eisenberg A 1995 Direct observation of 2 glass transitions in silica-filled polymers—implications for the morphology of random ionomers *Macromolecules* **28** 396–8
[26] Tsagaropoulos G and Eisenberg A 1995 Dynamic–mechanical study of the factors affecting the 2 glass-transition behavior of filled polymers—similarities and differences with random ionomers *Macromolecules* **28** 6067–77
[27] Wetzel B, Rosso P, Haupert F and Friedrich K 2006 Epoxy nanocomposites—fracture and toughening mechanisms *Eng. Fract. Mech.* **73** 2375–98
[28] Yong V and Hahn H T 2004 Processing and properties of SiC/vinyl ester nanocomposites *Nanotechnology* **15** 1338–43
[29] Zhao S, Schadler L S, Duncan R, Hillborg H and Auletta T 2008 Mechanisms leading to improved mechanical performance in nanoscale alumina filled epoxy *Compos. Sci. Technol.* **68** 2965–75
[30] Zunjarrao S C and Singh R P 2006 Characterization of the fracture behavior of epoxy reinforced with nanometer and micrometer sized aluminum particles *Compos. Sci. Technol.* **66** 2296–305